EUROfusion

EUROFUSION WPMAT-PR(15) 14622

M Roldan et al.

THE EFFECT OF TRIPLE ION BEAM IRRADIATION (Fe3++He++H+) ON CAVITES FORMATION ON PURE EFDA Fe.

Preprint of Paper to be submitted for publication in
Journal of Nuclear Materials

This work has been carried out within the framework of the EUROfusion Consortium and has received funding from the Euratom research and training programme 2014-2018 under grant agreement No 633053. The views and opinions expressed herein do not necessarily reflect those of the European Commission.

THE EFFECT OF TRIPLE ION BEAM IRRADIATION (Fe^{3+}+He^{+}+H^{+}) ON CAVITES FORMATION ON PURE EFDA Fe.

M. Roldán[1*], P. Fernández[1], R. Vila[1], A. Gómez-Herrero[2] and F.J. Sánchez[1].

[1]*National Fusion Laboratory-Fusion Materials, CIEMAT, 28040 Madrid, Spain.*

[2]*National Centre of Electronic Microscopy, Complutense University, 28040 Madrid, Spain.*

Abstract

Pure EFDA Iron was irradiated under triple ions beam (Fe+He+H) at 350 ºC, 450 ºC and 550 ºC to a nominal 40 dpa with an uniform He concentration of ~50 appm He/dpa and H content of ~14 appm H/dpa at depth between 1 and 2µm.

Cavity characteristics (size, morphology, distribution and population) at each irradiation temperature have been studied by TEM using FIB lamellae, showing bubble formation at all irradiation temperatures but with several differences. At 350 ºC homogeneous distribution of small cavities with sizes in the range from 2 to 4 µm was observed. However, irradiations at 450 ºC and 550 ºC lead to nonhomogeneous distribution of cavities with a wide range of sizes. In addition, at these temperatures it was detected preferential nucleation of bubbles within the ferritic grains exhibiting rounded and faceted shapes. Faceted cavities with sizes larger than 16 nm were detected at 450ºC and 550ºC.

**Corresponding Author*

Name: Marcelo Roldán

e-mail: marcelo.roldan@ciemat.es

Affiliation: National Fusion Laboratory-CIEMAT. Avda. Complutense, 40. 28040. Madrid. Spain.

1. INTRODUCTION

Nowadays, one of the most important challenges in the development of fusion energy is to predict and mitigate the effects of large levels of gas atoms transmuted (He+H) and displacement damage produced by high energy neutrons on the swelling and mechanical properties of the structural materials [1]. In fact, the He effects and their synergies with displacement atoms and H are still key a issue. The understanding of the macroscopic effects on cavity (bubbles, voids) formation due to He accumulation on the structural materials, requires many investigations at different levels; experimental observations by TEM in basic and simple metals (model alloys) and modeling. As a primary objective of such modeling and associated experiments, is to predict the dominant mechanisms controlling its generation, diffusion, kinetic of bubble/void nucleation and growth.

Different experimental approaches have been extensively used to study He effects for a wide variety of materials and conditions. The most notable irradiation techniques include multi-beam ion irradiations [2, 3] neutron irradiations in mixed fast-thermal spectrum fission reactor of alloys naturally containing, or doped with, Ni and B [4-6], in situ He implantation in mixed spectrum fission reactors [7] and spallation proton-neutron irradiations [8-10]. All of these methods present limitations and none of them simulate fusion neutron spectra. However, all these irradiation tools closely integrated contribute to understand the key role of He on void swelling.

Triple ion beams are very useful to explore mechanisms because the conditions can be well controlled and in many cases selectively and widely varied. This method based on carefully designed experiments (temperature, radiation damage, He/dpa and H/dpa ratios) is a very attractive approach to identify and quantify key processes to calibrate advanced physical models.

Tanaka's [11] experiment has been used during a long time as a model to understand the synergetic effect of triple simultaneous irradiation in steels (radiation damage + H + He). However some doubts appeared on repeated experiments (but unpublished ones) where these effects were not found and therefore creates the need to repeat this experiment in Europe to confirm or deny these results.

The objective of this work is to gain some insights about synergetic effects of the triple irradiation on microstructural evolution in order to provide reliable data to modeling.

2. EXPERIMENTAL

2.1 Material

The material investigated in this work is pure Iron fabricated under contract EFDA-06-1901. Details of fabrication, analysis and microstructural characterization are given in [12].This model alloy was delivered on recrystallized state after cold reduction of 70% and heat treated at 700ºC/1 h followed by air cooled, with the chemical composition indicated in Table 1.

Alloy	**C** ppm	**S** ppm	**O** ppm	**N** ppm	**P** ppm	**Cr** ppm
Fe	4	2	4	1	< 5	< 2

Table 1: Chemical composition of the pure EFDA Iron used in this work.

After the final heat treatment the material presents a mean grain size of 183 μm, but with minimum and maximum sizes of 4 and 650 μm, respectively. The dislocation density is very low, about 1.2 10^{8}cm^{-2} and its distribution is heterogeneous.

2.2 Triple ion beam (Fe^{3+}+He^{+}+H^{+}) Irradiation

The triple irradiation was carried out at the Joint Accelerator for Nanosciences and Nuclear simulation (JANNUS) located at CEA Saclay (France).

The simulation was carried out by using full cascades mode in SRIM with a displacement energy for Fe atoms of 40 eV [13], in order to calculate the total vacancies produced by the irradiation.

In a first step, the irradiation was designed to use a beam degrader with the three beams in order to simulate the fusion environment over the depth range from 1 to 2 μm, using implantation energies of 10 MeV (Fe^{3+}), 1.3 Mev (He^{+}) and 600 KeV (H^{+}) to produce damage of ~ 40 dpa, ~500 appm He and ~ 2000 appm H. The dpa contribution arising from He and H implantation were negligible compared to that of the Fe ion whose damage rate at the peak was around 1.7x10^{-3} dpa/s for all the irradiations. This irradiation configuration leads to He/dpa and H/dpa ratios of ~12.5 and ~50, respectively. Unfortunately during irradiation at 550ºC some Al foils of Fe beam degrader were destroyed due to the iron beam flux and it was decided to perform the Fe^{3+} irradiation without beam degrader in the other temperatures (350ºC and 450ºC) but using two individual energies of 5 and 10 MeV with a flux ratio of 1:3. With this new implantation configuration the damage level and the He/dpa and H/dpa ratios were practically the required ones; 40 dpa, ~14 He/dpa and ~50 H/dpa (Figure 1). The irradiation was carried out on 3 mm diameter disks of pure Fe.

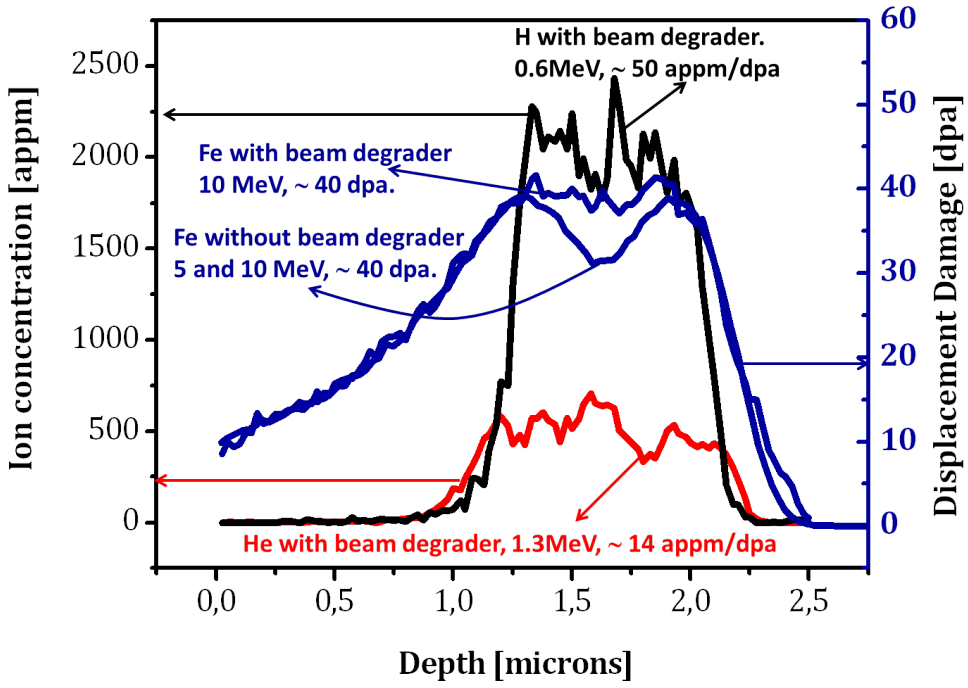

Figure 1: SRIM calculation for triple ion irradiation at Jannus on pure Fe.

2.3 Microstructural characterization

A Zeiss Focused Ion beam (FIB) microscope was used to micro-machine thin transparent lamellas, which included both damaged-implanted and undamaged regions. The extracted lamella was thinned in different paths (Figure 2) in order to study the homogeneity of the nucleation defects. The microstructure of each path was studied separately at different lamellae and the implantation depth (2 m) was divided into bins of 250 nm to do the calculus.

TEM observations were performed on a JEOL JEM 2100 and JEOL JEM 3000F operating at 200 and 300 kV respectively. Cavities were characterized by through-focus bright field sequence method with the specimen tilted away from the Bragg condition in order to avoid as much as possible the orientation contrast which making the cavities observations impossible. The magnification was adjusted to provide the optimal visibility for each irradiation temperature. All the detected cavities were measured (by using an image software) and located with respect to the irradiation surface. The foil thickness of each lamella path was calculated by convergent beam electron diffraction (CBED) as shown in Figure 2. Finally the number density and swelling (in terms of volume fraction) per bin were calculated.

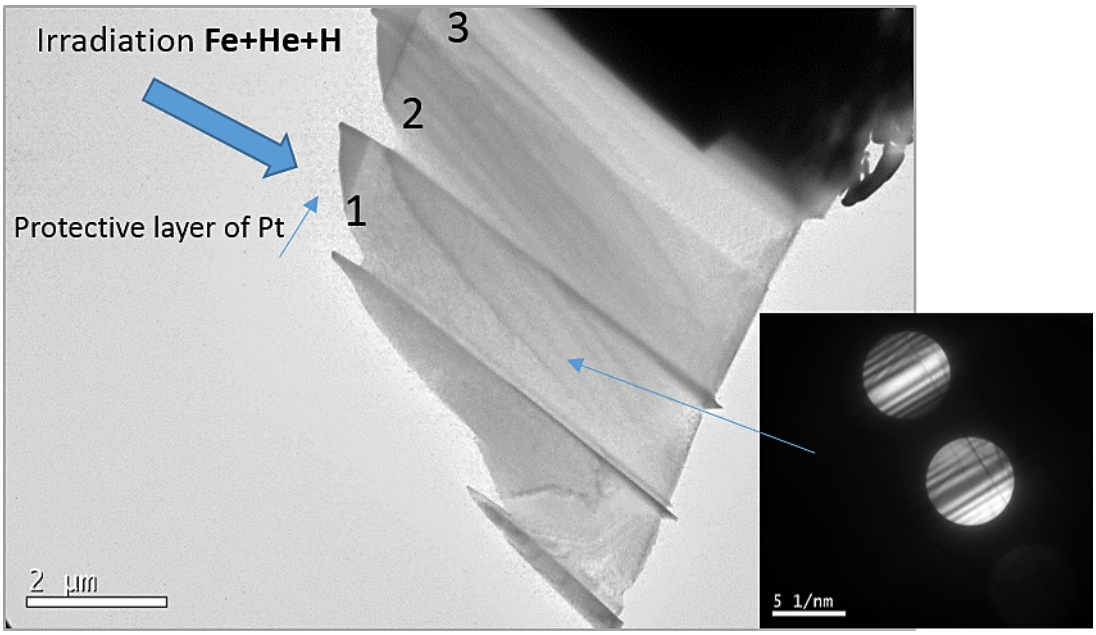

Figure 2: Lamella of UHP Fe showing 3 paths (numbered from 1 to 3) with their characteristic thickness measured by CBED (one of them is showed as example).

With this methodology was possible to obtain a large enough TEM observable area and hence a very good statistics.

It was not determined whether the cavities observed were filled or not with Helium, so as the ratio He/V and cavities pressure remains unknown it is not possible to distinguish if the defects were bubbles or voids, hence in this paper were called just cavities.

3. RESULTS

3.1 As received condition

Due to the importance of the microstructure previous to the irradiation it is necessary to perform a TEM analysis on some UHP Fe samples in order to analyze the dislocation density and any other microstructural features which were able to interact with the irradiation defects.

The sample of UHP Fe was cut and thinned up to less than 100 m thickness, then it was punched out into a 3 mm disc. Finally it was prepared by electropolishing with TENUPOL device using H_2SO_4 (20%) and methanol (80%) at 15 ^oC and around 9 V.

The dislocation density was calculated using the mean interception length method with 5 lines per micrographs. In order to obtain random images, the micrographs used were the ones taken from the areas located around the transparent hole each 45^o (in Figure 3 a) and b) is possible to see two of the ones used for the calculus) in a bright field imaging condition and random crystal orientation.

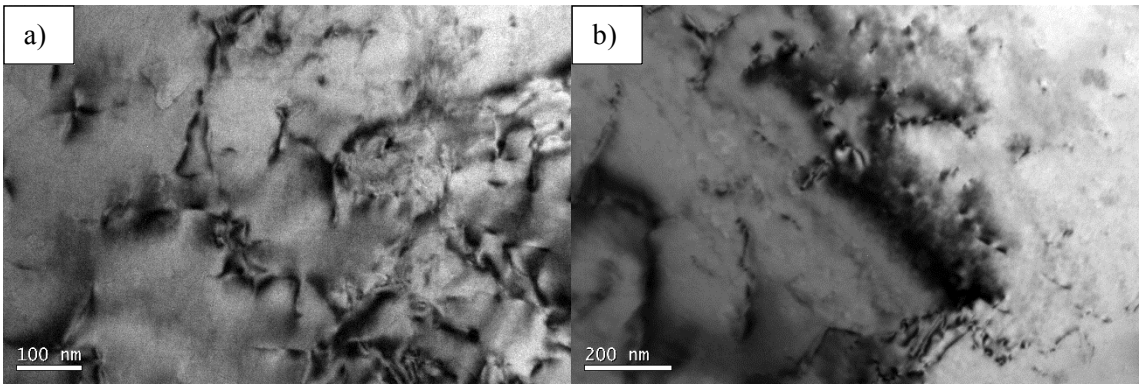

Figure 3: TEM micrograph of EFDA Fe in as received condition showing some dislocations, at two different positions, a)90 degrees and b)180 degrees around the hole.

The TEM observations are in good agreement with the manufacturer report [12] except in the dislocation density number, that it was $\rho = 1.44 \times 10^{10}$ cm^{-2} for the as received condition just before the irradiation. This number is 2 orders of magnitude larger than the value given for the manufacturer.

3.2 Irradiation at 350ºC

The different paths of the lamella extracted from the pure Fe specimen irradiated at 350 ^{o}C with triple ion beam were analyzed searching cavities nucleated from the very surface up to 2.25 μm in depth. At this irradiation temperature all the cavities showed a round morphology with random distribution within the matrix. Regarding cavities diameter, their size depends strongly on the lamella depth. First of all, many cavities were detected very close to the irradiated surface up to the first 500 nm, whereas the population starts decreasing until 1 m (Figure 4). At a deeper position, cavities were detected, but they are very small.

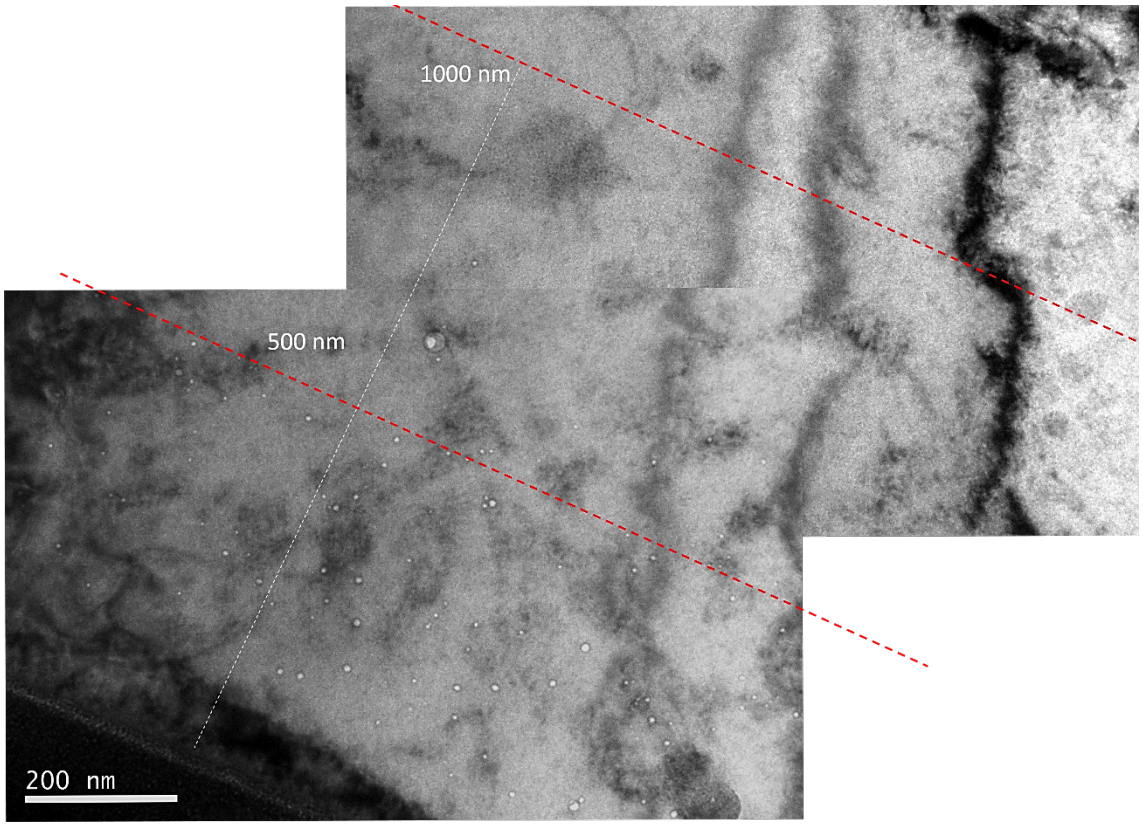

Figure 4: Under-focus TEM images of pure Fe irradiated with triple ion beam up to 40 dpa, ~14 He/dpa and ~50 H/dpa at 350ºC. Cavity distribution from the surface up to 1 m.

The cavities population suddenly increased at 1.5 m as can be seen in Figure 5. However, although the amount of cavities raised, the impact on swelling is very low, since the maximum measured diameter of those cavities was less than 5 nm.

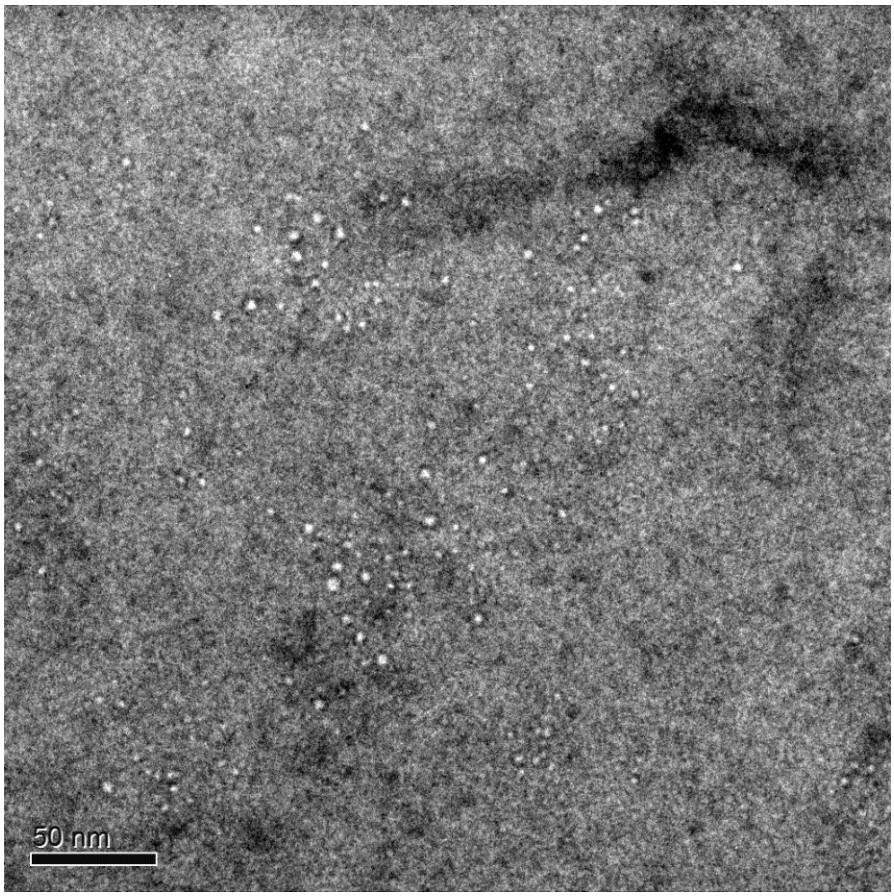

Figure 5: Under-focus TEM micrograph of pure Fe irradiated with triple ion beam up to 40 dpa, ~14 He/dpa and ~50 H/dpa at 350ºC. Cavity distribution at 1.5 m far from the surface.

Pure Fe irradiated with triple ion beam at 350ºC showed cavities distributed within the matrix with a wide range of diameters from 1 nm up to 18 nm maximum. Analysis of images taken along the irradiated region showed that most of the largest cavities (≥ 4 nm) are located between 0 and 500 nm, but they were also found at larger depths (Figure 6 a). As can be seen in this figure, beyond that depth the population number density increases as the size decreases, reaching a nucleation maximum of ~3.5×10^{22} m^{-3} at 1500 nm as seen in Figure 5. Taking into account the SRIM calculation (Figure 1), it would be expected that the largest cavities were located between 1 and 2 microns due to reported synergistic effects between He and H, together with the maximum dpa value. Although cavities with a wide range of sizes were detected and measured, from Figure 6 a) it can be deduced that the largest population densities corresponds to sizes lower than 2 nm and sizes between 4 and 6 nm. It is clear that the irradiation conditions performed in this work at 350ºC produced bimodal range of cavity diameter. Figure 6 b) shows the corresponding variation of volume fraction in function of implantation depth. Note that the swelling is very low since it did not exceed 0.2%, indeed the maximum value in population density has not much influence on swelling due to the size of the cavities.

The cavity number density indicates the cavity population per m^3, Figure 6 c), which shows an increasing trend as the irradiation depth increases with a maximum between 1500 to 2000 nm according to the maximum damage area.

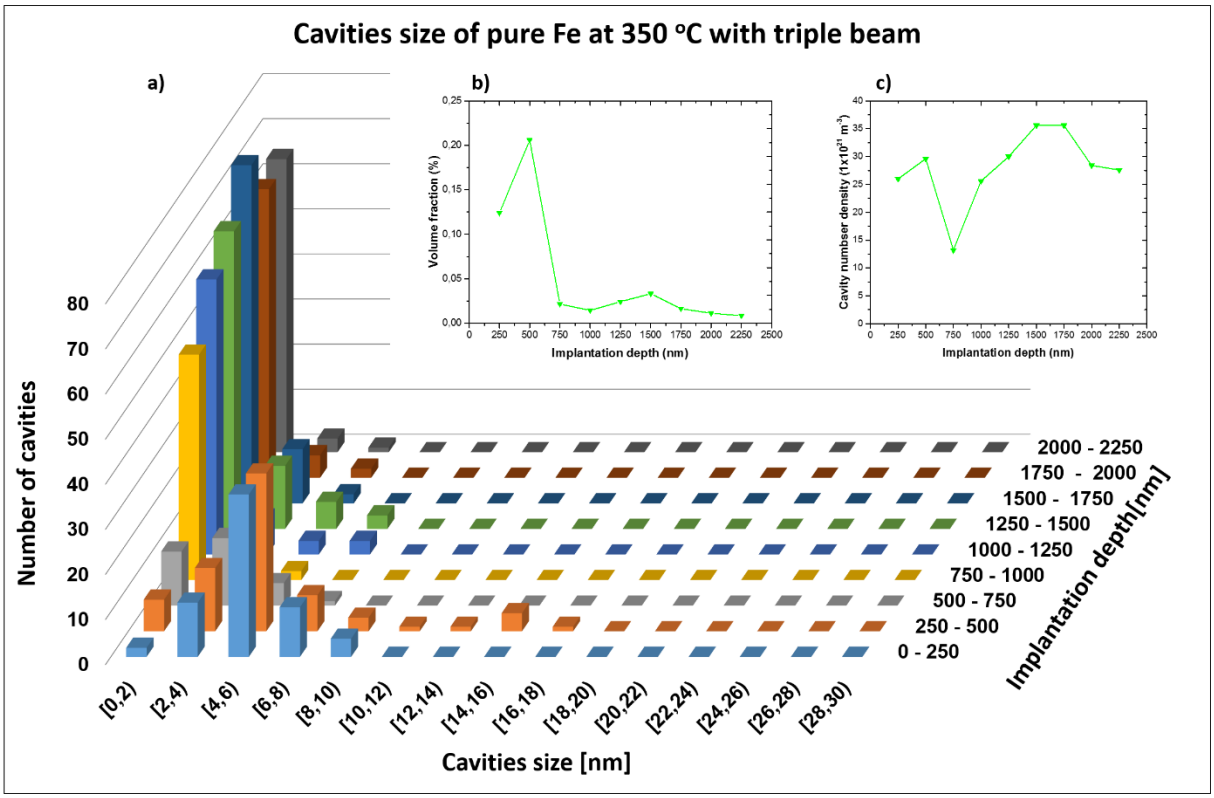

Figure 6: a) Cavity size and b) Volume fraction in function of irradiation depth and c) cavity density number of pure EFDA Fe irradiated by triple ion beams to 40 dpa, ~14 He/dpa and ~50 H/dpa at 350ºC.

3.2 Irradiation at 450ºC

At this irradiation temperature, the cavities are non-uniformly distributed, exhibiting preferential formation with round and polyhedral-faceted shape, unlike the cavities detected in the specimen irradiated at 350 °C which are all round. Figure 7 shows the overview of the irradiation depth from the very surface up to deeper than 2 m. Most of the cavities regardless their size, nucleated following a determined arrangement. Increasing the magnifications it is possible to observe with more detail some different clusters of cavities nucleated approximately at 1 m further from the irradiated surface (Figure 8 from the red rectangle in Figure 7). The mentioned picture shows clearly how the clusters have two different average sizes, which means the large cavities coexist with cavities with similar size and vice versa. This heterogeneous distribution is probably due to the interaction between local variations in the microstructure such as dislocations (which were detected on the as received condition) or even grain boundaries with the cavities, which can interfere on nucleation.

Those microstructural characteristics may be invisible under the TEM operation conditions used in this work to identify the cavities.

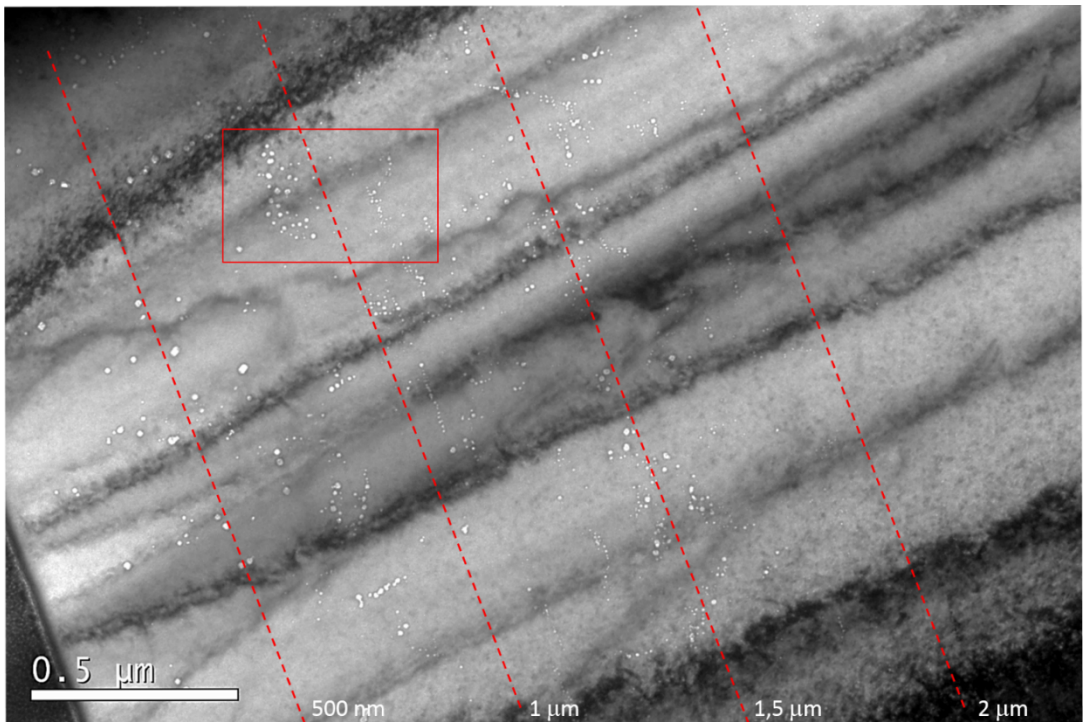

Figure 7: Bright field TEM image showing the cavity distribution, size and morphology on pure EFDA Fe irradiated by triple ion beams to 40 dpa, ~14 He/dpa and ~50 H/dpa at 450ºC.

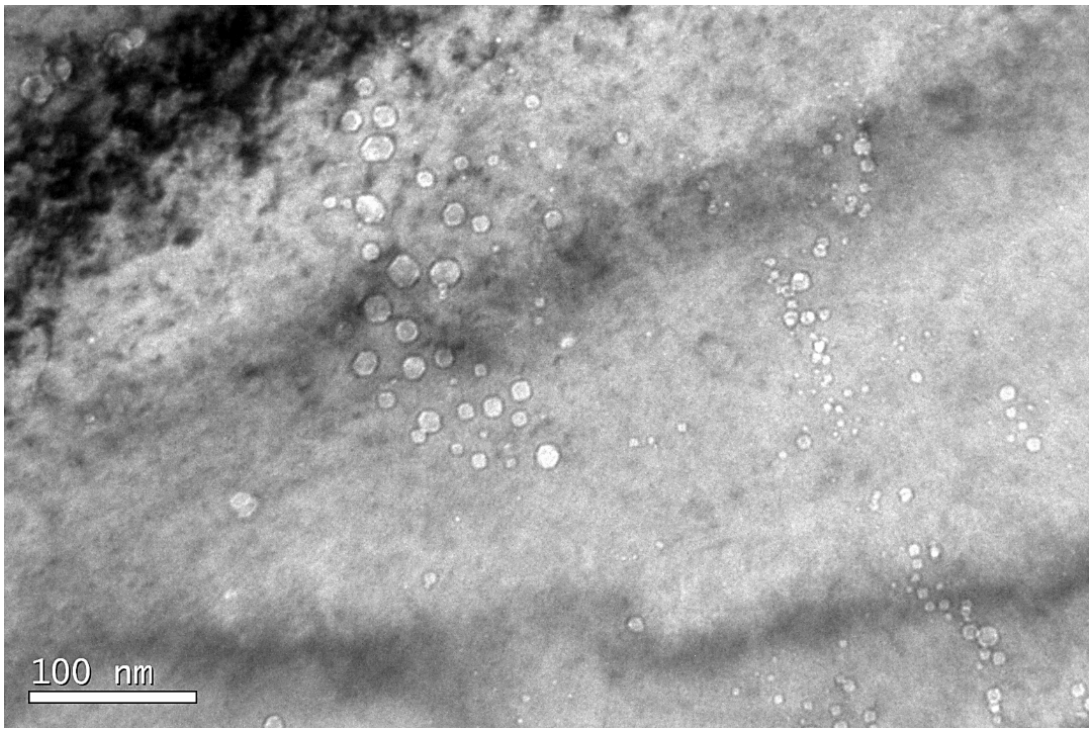

Figure 8: Bright field TEM image showing different clusters of cavities on pure EFDA Fe irradiated by triple ion beams to 40 dpa, ~14 He/dpa and ~50 H/dpa at 450ºC.

As a result of the analysis of the whole irradiated zone at 450 ºC (Figure 9), the cavities showed a wide range of sizes from 1 up to 18 nm. As the depth of implantation increases, a few cavities with sizes around 20 nm were also detected. The largest cavities (≥ 4 nm) were observed within the damage region from 500 to 2000 nm. The most common diameter range detected was the one between 2 and 4 nm. Figure 9 b) shows the changes in volume fraction of the cavities in function of the implantation depth. As can be seen, at 450ºC the swelling remains low, but in comparison with the irradiation at 350ºC, the irradiation temperature increment of 100ºC enhances the swelling up to approximately 1.2%. The cavity population increases rapidly up to 750 nm, and also their size do, suggesting the bimodal bubble-void transition. But then both parameters decrease gradually, reaching another minimum out of the irradiation peak. This fact is observed according to the density cavity number, Figure 9 c).

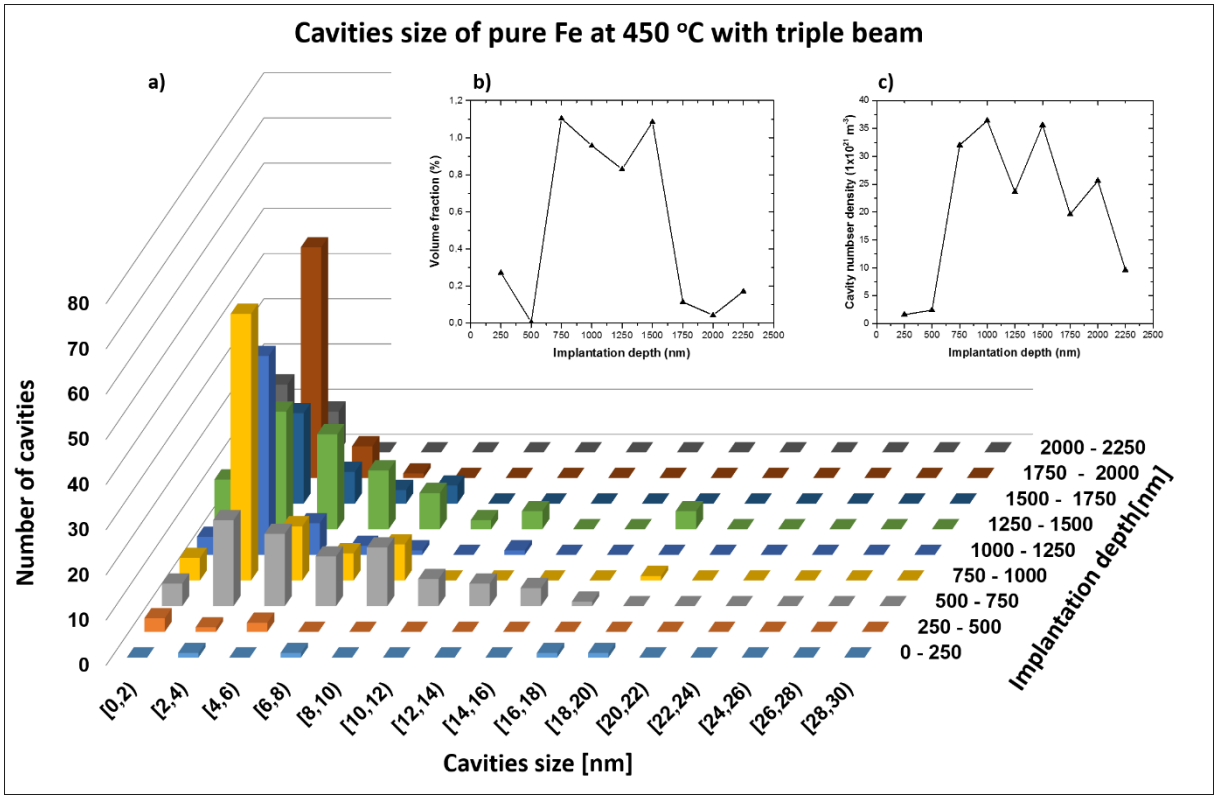

Figure 9: a) Cavity size and b) Volume fraction in function of irradiation depth and c) cavity density number of pure EFDA Fe irradiated by triple ion beams to 40 dpa, ~14 He/dpa and ~50 H/dpa at 450ºC.

3.3 Irradiation at 550ºC

The last pure Fe specimen analyzed was the one irradiated at 550 °C. Cavities were observed from the implanted surface up to 2250 nm, with different size and population density depending on the location on the damaged region. After an exhaustive analysis by TEM of each lamella path of this specimen, the observations indicated that the number of cavities nucleated between the surface and

500 nm are low as well as their size comparing this sample with the other irradiation conditions. The maximum size measured in this region was 4 nm. From that depth the cavities experimented a growth in population and mainly, regarding swelling, in size. An overview of one of the path is presented in Figure 10 which characterizes all the irradiation damage area from the surface up to 2 m and represents the aforementioned cavities characteristics. With regard to the shape, cavities detected presented both round and polyhedral-faceted shape (Figure 12), as in the case of irradiation at 450ºC.

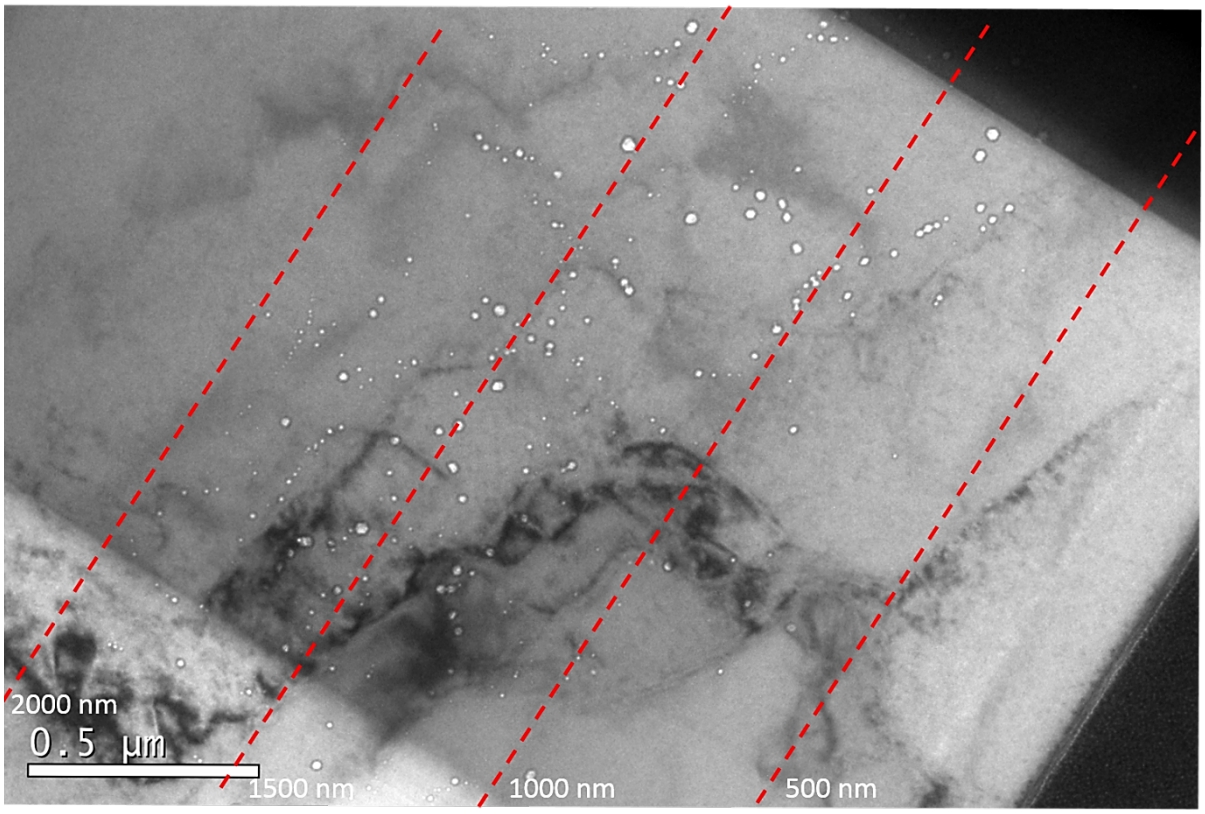

Figure 10: Overview of the irradiation area from one lamella path extracted from the specimen irradiated with triple beam at 550 ^{o}C

The population and cavity size in function of the implantation depth is shown in Figure 11 a). From this figure, it is deducible that the maximum population of cavities exhibiting sizes ≥ 4 nm is mostly placed inside the damage peak which is located between 1 and 2 m depth. The highest irradiation temperature clearly leads to an increase of the cavity size. Large faceted cavities from 6 to 30 nm have been detected between 750 and 1500 nm. At this irradiation temperature, the maximum volume fraction calculated was 1.4 %, obtained at 1250 nm (Figure 11 b). Clearly, the effect of large cavities on swelling is critical compared with many small cavities. Although this value is the highest swelling rate of the three irradiation temperatures is still low if it is compared with another triple beam experiments [11]. Regarding the cavity number density, this value increases as the irradiation depth increases as well, achieving its maximum at 1500 nm, ~2.5x10^{22} m^{-3}.

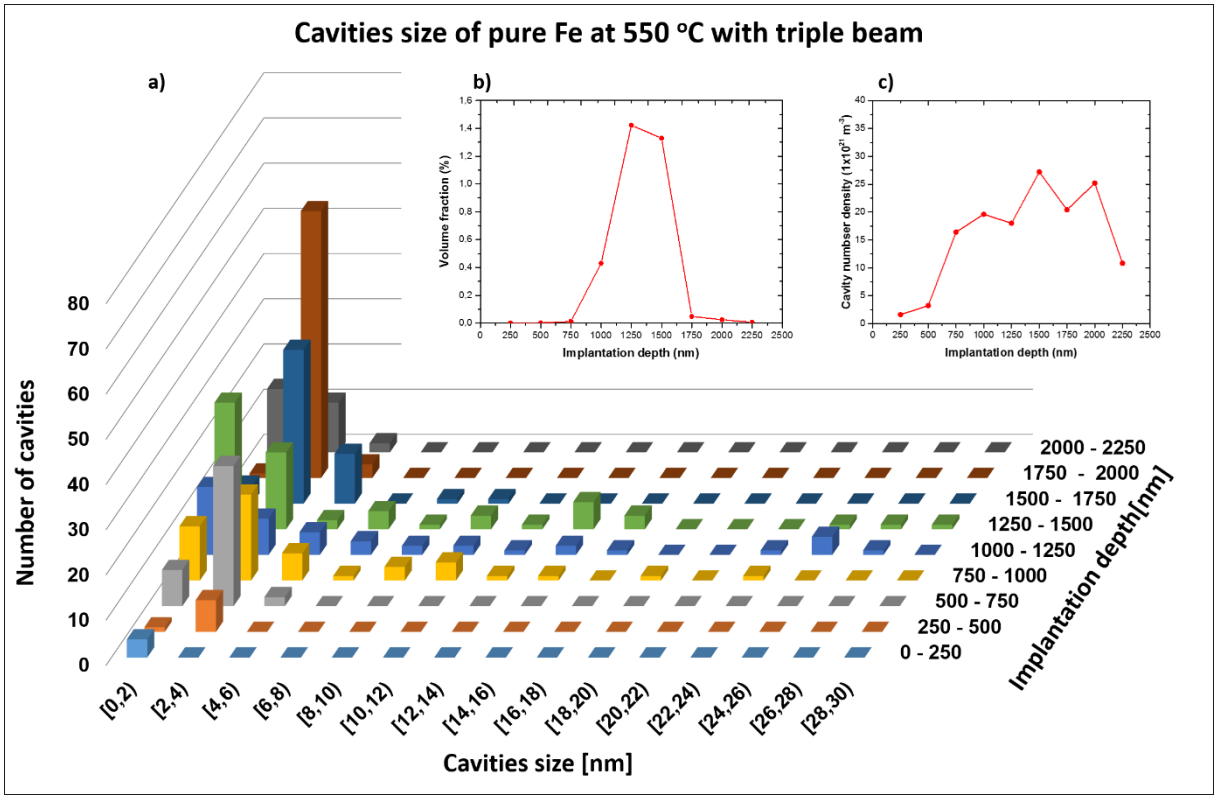

Figure 11: a) Cavity size and b) Volume fraction in function of irradiation depth and c) cavity density number of pure EFDA Fe irradiated by triple ion beams to 40 dpa, ~14 He/dpa and ~50 H/dpa at 550ºC.

At 1250 nm the maximum swelling value was obtained as well as the largest cavity detected, ~30 nm. It corresponds with maximum He/dpa and H/dpa ratio and maximum dpa level. Figure 12 shows in a more detailed way, some micrographs taken from that very depth where it is possible to see the alignment of the cavities along dislocations or grain boundaries likewise the size distribution. The nucleation is completely preferential regardless of the size.

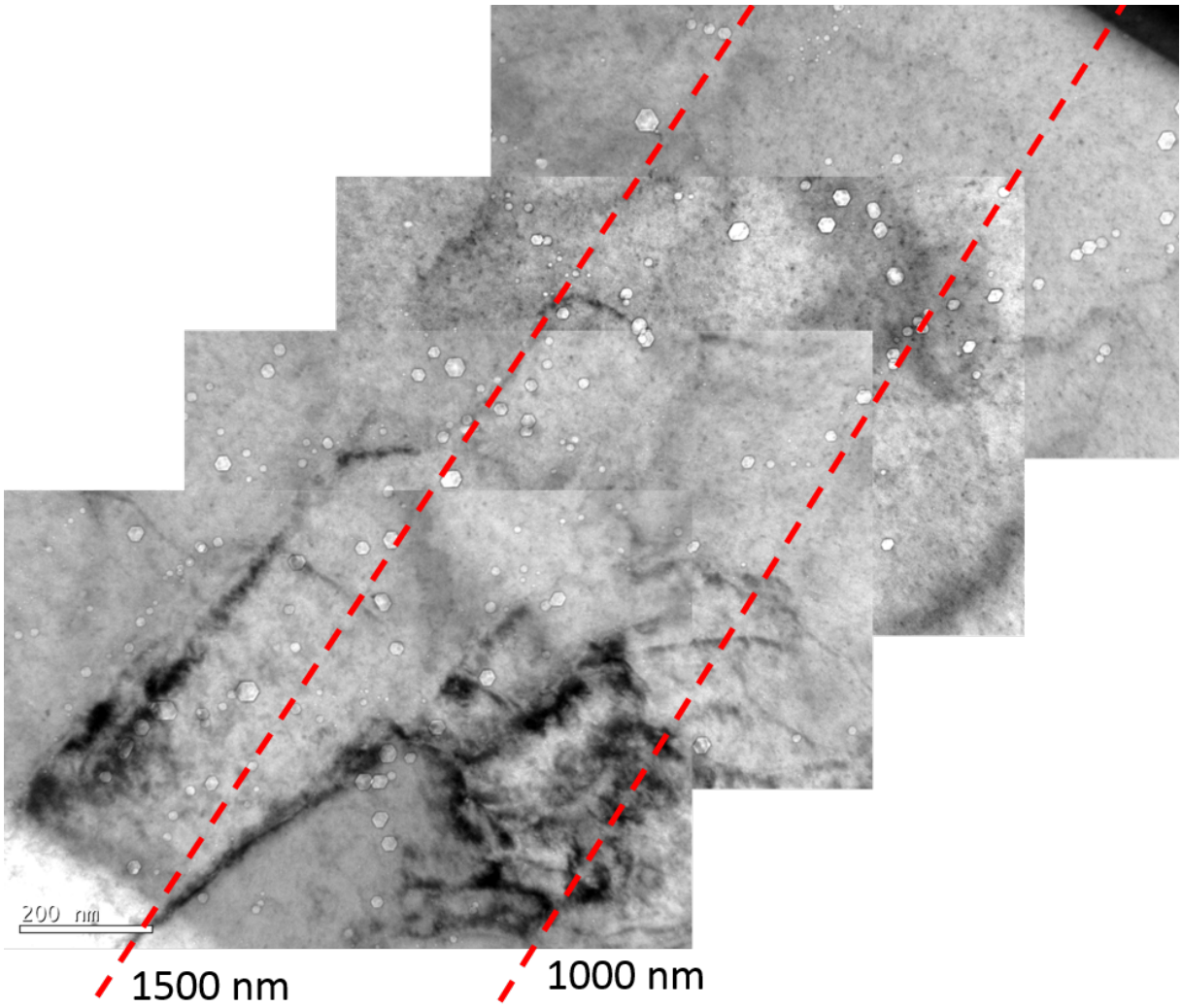

Figure 12: Detail of the cavities distribution on pure EFDA Fe irradiated by triple ion beams to 40 dpa, ~14 He/dpa and ~50 H/dpa at 550°C taken from 1 to 1.5 m depth.

4. DISCUSSION

As shown in Figure 6, Figure 9 and Figure 11, the cavities, regardless diameter, have been detected out of the damage peak (confined between 1 and 2 µm, Figure 1) for all the irradiation temperatures. Those observations indicate that the nucleation depends strongly on irradiation temperature as well as the peak swelling does.

A well-known effect, called interstitial injection, is observed when Fe ions used as displacement cascades producers act as interstitials at their stopping range which strongly decrease the void nucleation and growth [14-16]. Only taking into account the Fe implantation, the material showed an area rich in vacancy up to the first micrometer in depth and an area richer in interstitials due to the injected Fe ions deeper than 1 m, as seen in Figure 13. The contribution of He and H on cavities fate (nucleation, growth and distribution) complicates the picture, since binding and diffusion energies play an important role, especially after 1 m depth when either He and H were introduced.

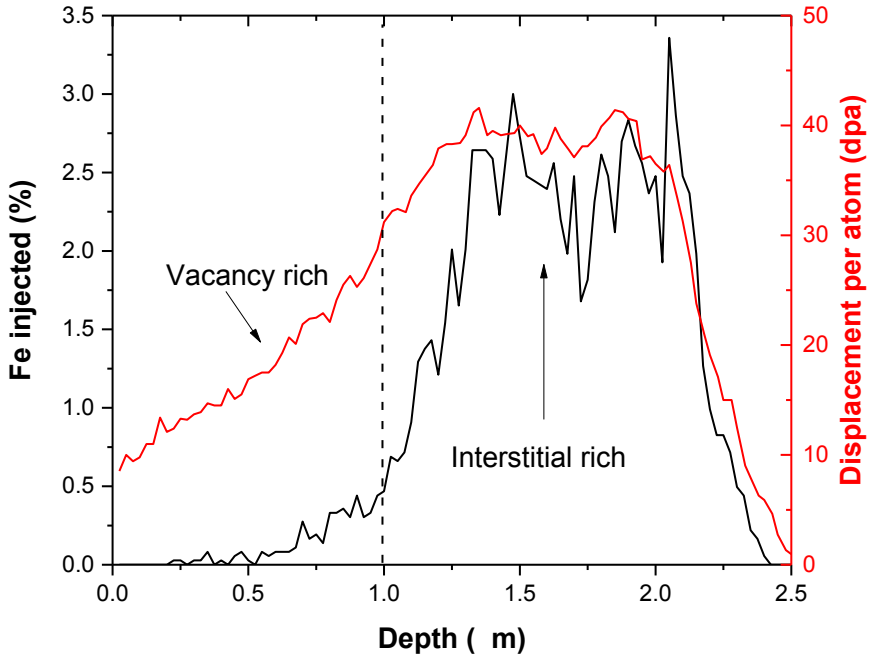

Figure 13: Depth distribution of vacancies in terms of dpa and interstitial generated by Fe ion beam.

Figure 14 showed the comparison in volume fraction (a) and in cavity number density (b) for all the irradiation temperatures. In each figure was included the irradiation profile, except the injected interstitials profile seen in Figure 13, in order to get a better visualization. In those figures is possible to see that at 350ºC the swelling peak, 0.2 %, is located at a depth about 500 nm, then there is a suppression of nucleation of larger cavities, enhancing only the nucleation of the smaller ones. At 1500 nm the specimen showed other increase in swelling (~0.03 %) but this value is much smaller than the peak mentioned above.

As the irradiation temperature increases the swelling peak moves deeper into the material likewise increasing its value. At 450 ^{o}C it was measured a large value of swelling at 750 nm, possibly due to some large cavities (between 8 and 18 nm) detected in the matrix. Iit is possible to explain this result due to the high amount of vacancies created by the Fe beam without He and H, whose diffusion is enhanced by temperature. In fact, at this point the swelling value is the largest measured, 1.1 %, another swelling peak is detected deeper, but is slightly lower, 1.08 %, anyway it was not expected such a highest value, but something smaller which followed the ascending trend in a similar way to the 550 ^{o}C swelling profile.

The specimen irradiated at 550 ^{o}C showed the maximum swelling value at 1250 nm which was of 1.42 %. Then, like the other experiments reduced the nucleation of large cavities as well as the population. In any case, the swelling measured in this research is far from the common value of swelling for ferritic-martensitic materials, which is ~0.1 %/dpa [17].

If the irradiation profile is taken into account up to 1 m (where the gases injection is almost negligible), there is a peak swelling due to the nucleation and growth of voids whose maximum was at 450 ^{o}C. Moreover, focusing on the swelling peak at 250 and 2250 nm, again with no influence of gases, there are another two swelling peaks at 450 ^{o}C. Clearly the values are much lower, only 0.27 and 0.17 % respectively but the dpa values at those depths are lower than 20 dpa.

On the other hand, analyzing the profile between 1 and 2 m the maximum peak is produced at 550 ^{o}C specimen, but at the three temperatures, each one showed a peak. Due to the evolution of the microstructure it is believed that the cavities detected there are HeV clusters even when the injected interstitials, showed in Figure 13, were placed and the recombination between those interstitials and the vacancies is maximum.

Regarding cavity number density, all the irradiations showed an increase in population, but depending on the temperature the growth will be enhance or not.

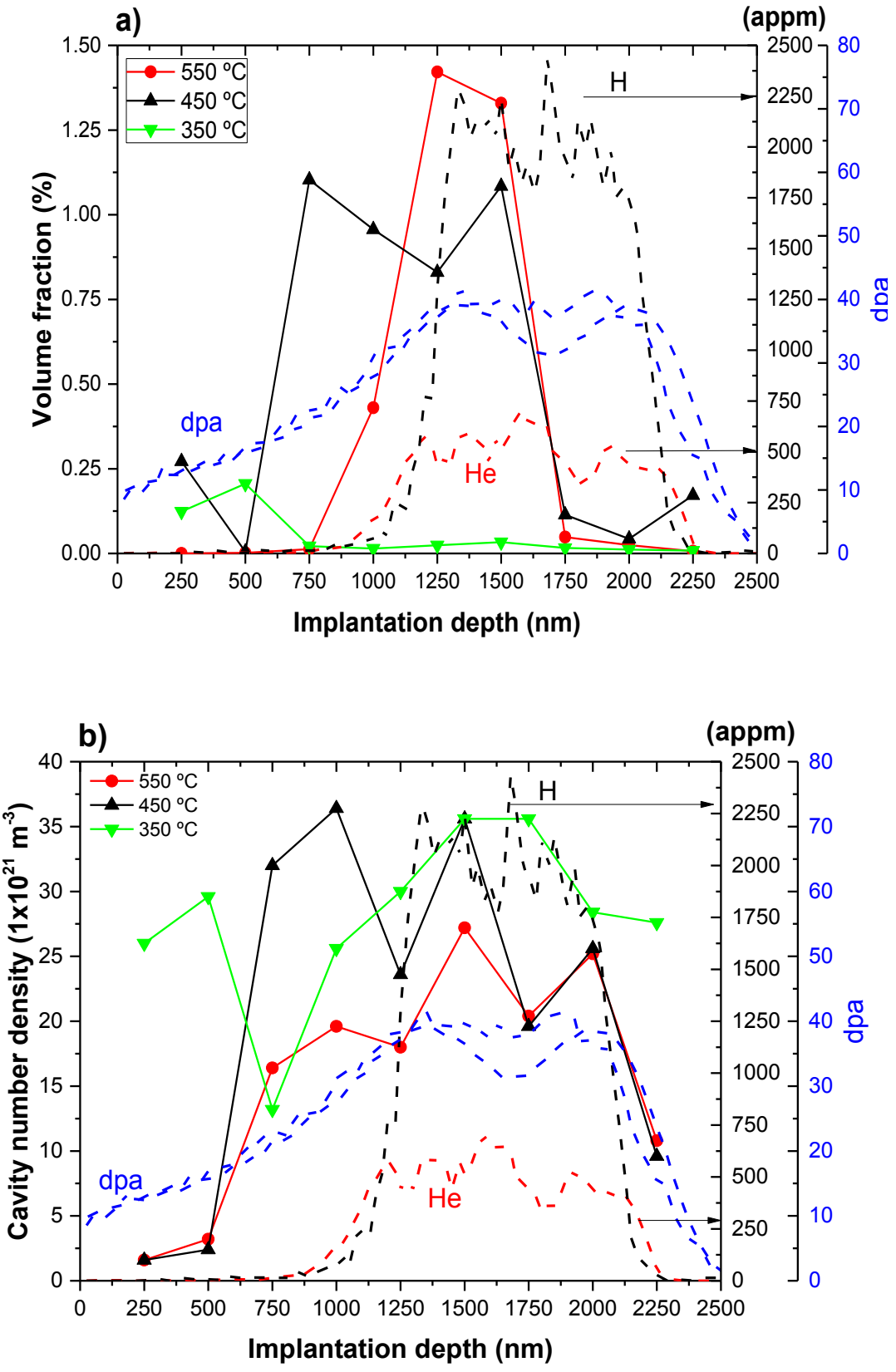

Figure 14 a) Volume fraction and b) cavity number density of UHP Fe irradiated at 350, 450 and 550 °C with $He^{+} + H^{+} + Fe^{3+}$.

Tanaka et al. [11] measured a maximum swelling of almost 4 % produced in the irradiation at 510 ^{o}C on Fe12%Cr model alloy. Comparing to UHP Fe, it turns out a large increase even when Tanaka irradiated a Fe12%Cr which, in theory, is more resistant to irradiation swelling. This phenomenon could be explained taking into account the Tanaka's irradiation profile. In their experiment light ions (He+H) were introduced before injected self-ions which produced an increase of recombination of vacancy-interstitial that reduces the swelling value. That fits with the observations extracted from this research if only the irradiation profile of this research is studied up to 1 m.

Regarding preferential nucleation, two clear features were observed. First of all the differences on cavities nucleation close to the irradiation surface according to the irradiation temperature. After an exhaustive microstructural analysis of the very surface (first 250 nm) of the irradiation depth of each specimen, it was observed that there is a clear variation in both nucleation and size depending on the temperature which was the only difference between the 3 specimens (and of course the change in irradiation setup, although the dpa, He and H levels were maintained at the same depth).

At 350 ^{o}C the observations revealed many cavities nucleated very nearby the surface, Figure 15 a), in fact at this depth this specimen had the highest cavity number density, 2.6×10^{22} m^{-3}. In contrast, at 450 and 550 ^{o}C in spite of having the same cavity density number, the size at 450 ^{o}C is higher, as seen in Figure 15 b) with cavities of 17 nm.

This phenomenon could be attributable to an unexpected local high dislocation density close the surface or simply to a heterogeneous nucleation due to the irradiation characteristics. For these irradiation conditions the surface effect acting as vacancy source [18-20] did not give a possible explanation, since the ions used are very energetic and the penetration reaches more than 2 m to be influenced by the surface.

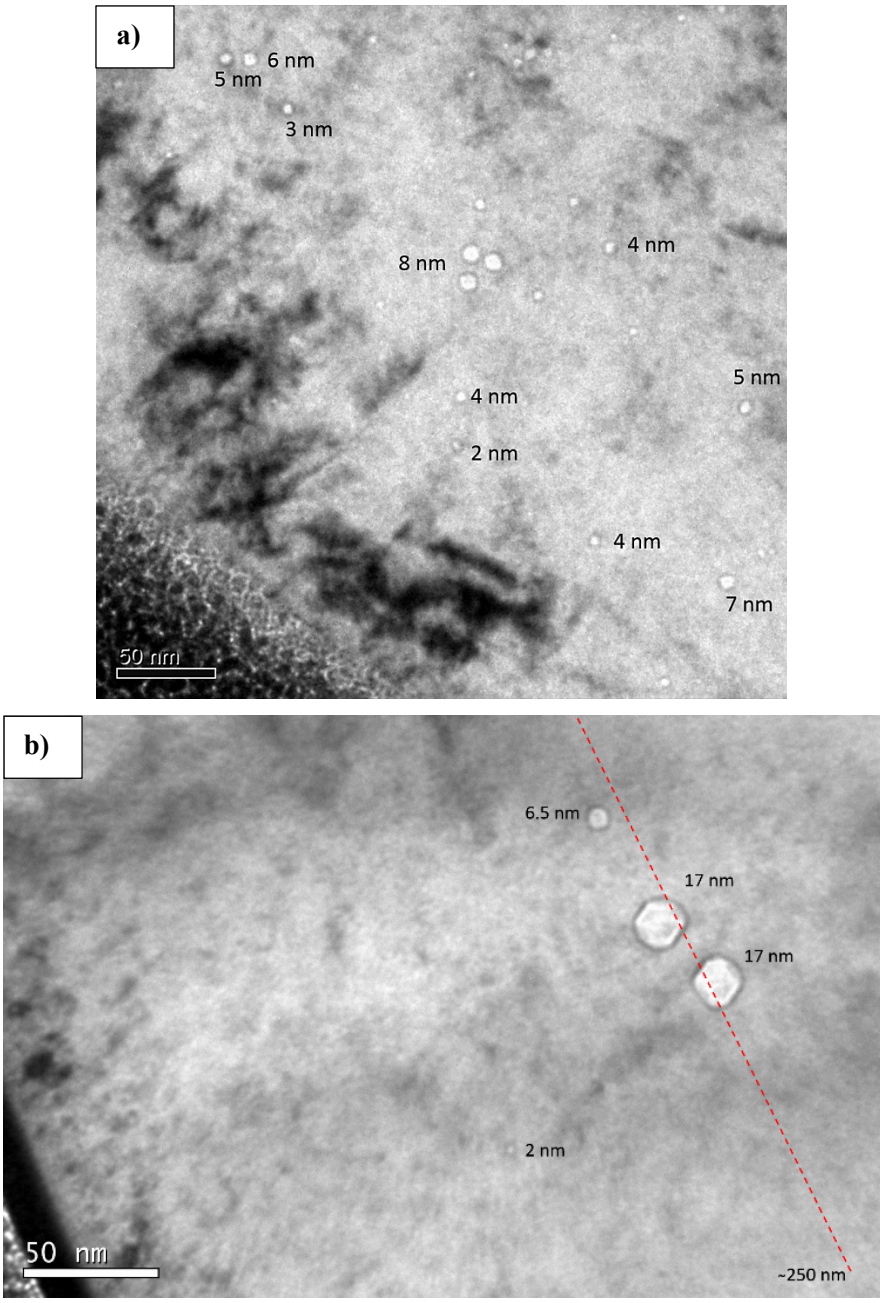

Figure 15: TEM micrograph of Fe UHP irradiated at a) 350 °C and d) 450 °C showing cavities nucleated very close to the surface.

On the other hand it is proved that an irradiation using defocused beam, produces a microstructural evolution more similar to that produced by the neutron irradiation than employing raster beams with certain sweep frequency [21, 22]. The irradiation at Jannus facility was performed using three defocused beams, so in order to make more comparable between neutron and ion irradiation (recognizing that the cases are not exactly the same) it is very important to try to avoid as much as possible undesirable effects. However, due to the high complexity of the experiment is possible to produce a nonhomogeneous nucleation.

The second feature observed was the nucleation on microstructural characteristics such as dislocations and grain boundaries. The effect of dislocations on cavity nucleation has been observed experimentally under triple beam irradiation, with a cold rolled specimen that showed more resistance to irradiation swelling than other specimens in as received condition [23]. That effect is explained easily by enhancing of trapping point defects.

The results of this research revealed that the irradiation at 350 ^{o}C does not produce a clear alignment of cavities. However with these experimental conditions at 1.5 m was observed a cluster arrangement nucleation (Figure 5) but it was not close to the surface (Figure 4) where the cavities nucleated randomly. So, the nucleation and growth mechanism seems to be different depending on the irradiation damage and temperature. On the other hand at 450 ^{o}C the nucleation in clusters is more significant than for the previous temperature as seen in Figure 7. Finally, at 550 ^{o}C the cavities showed a clear alignment along grain boundaries and probably dislocations, as shown in Figure 16 within the red rectangle. The largest ones also were aligned but due to its size is more difficult to notice.

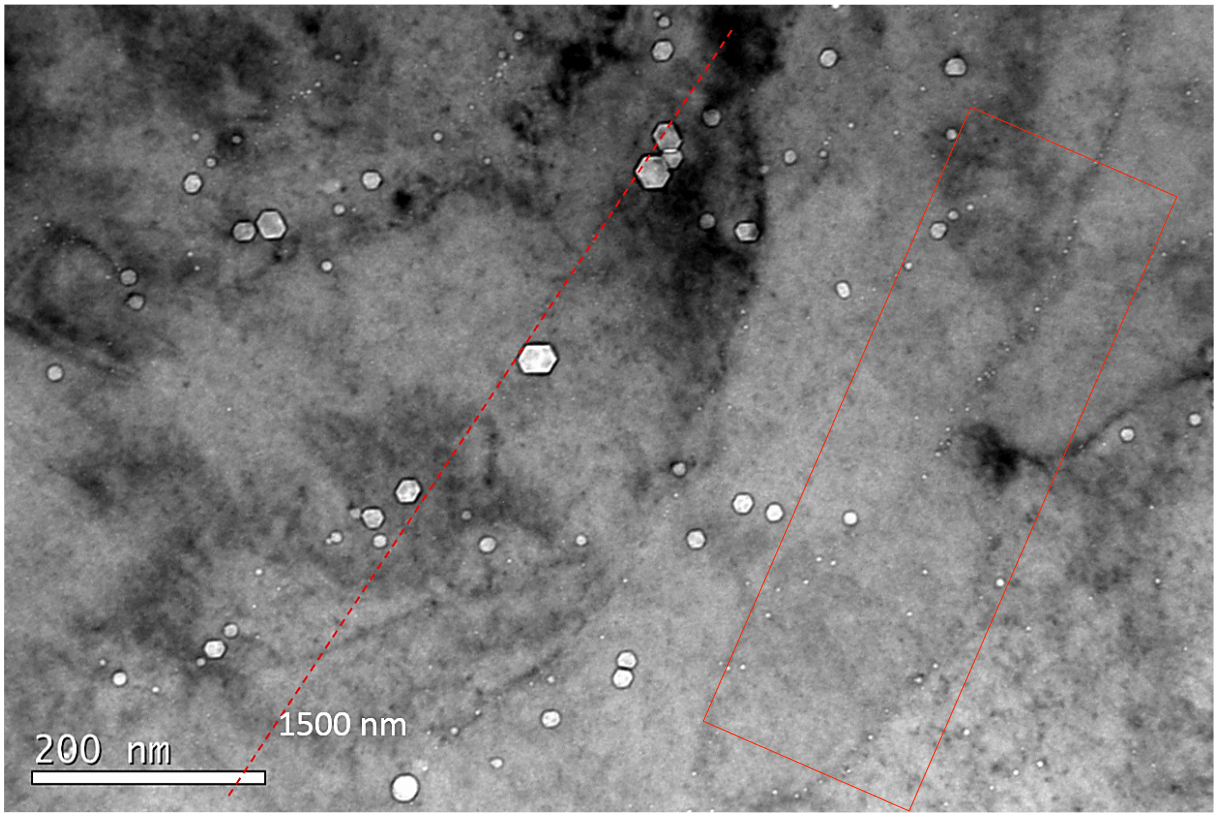

Figure 16: TEM micrograph taken from the specimen irradiated at 550 ^{o}C showing sub-grain structure whose boundaries are decorated with very small cavities, highlighted by a red rectangle.

Other interesting feature is the fact that there is a clear depletion of small cavities nearby the large ones at 450 and 550 ^{o}C, which seems to indicate a resolution of the small ones where are close or around larger ones. As example of the aforementioned, in Figure 17 (highlighted with red arrows) and Figure 18 it is possible to observe large and medium size cavities with very small cavities around of

them at 450 °C and 550 °C respectively. This phenomenon is called Ostwald ripening [24] and it is observed when large bubbles increase their diameter as the smaller ones decreases or even disappear by resolution of those ones.

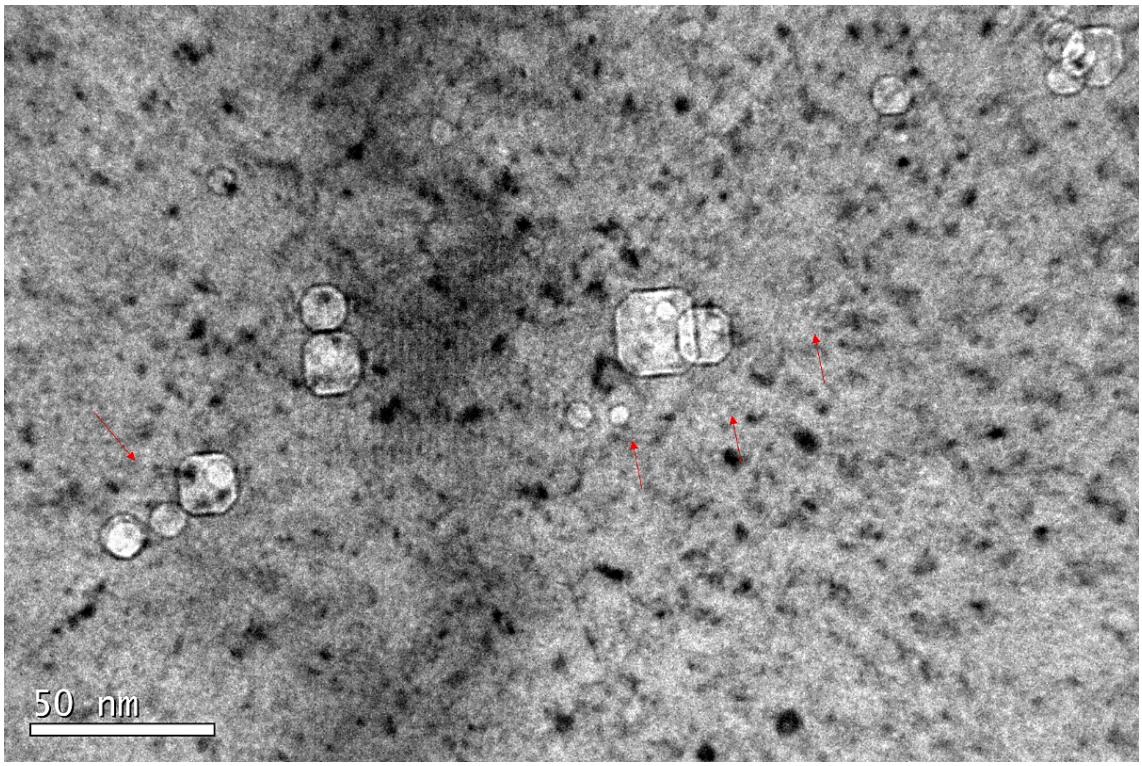

Figure 17: TEM micrograph of pure Fe irradiated with triple beam at 450 °C showing a resolution and growth of cavities.

Regarding the cavities shape, since the growth is affected by irradiation temperature it was also found that depending on that parameter the cavities will present round or polygonal faceted. At 350 °C all the cavities observed were round with a maximum size of 18 nm. At 450 °C, cavities of different shapes coexisted, being the largest round one detected of 21 nm, and the smallest faceted one had a diameter of 17 nm. Finally at 550 °C the largest one was faceted-like with a size of 30 nm (Figure 18), the smallest faceted one was 15 nm and the smallest diameter of a round cavity was 17 nm. These observations lead to think that 16 to18 nm is the limit diameter at which the cavity shifted its shape from round to polygonal. It is believed that the evolution of the cavity shape is related to the thermodynamic equilibrium between the superficial pressure of the cavity and the matrix, besides it is well-known that the internal pressure of a cavity depends completely of the ratio He/V. So, the following steps of this work is to try to measure the amount of He/H ratio and the cavity pressure to distinguish between void and bubble, using techniques such as EELS [25, 26]. In contrast to He that can be analyzed on HRTEM by EELS (Ref.), the H study require the other techniques such as Positron Annihilation Spectroscopy (PAS) [27] or by means of a nuclear resonance reaction after the irradiation

[23], but taking into account always that most of it probably release the specimen due to its high diffusivity, especially at high temperatures.

In fact, Frechard et al. [25] found a linear relationship between pressure and density of He atoms on bubbles which decreases significantly up to bubbles with a radio of 5 nm in an He implanted steel. Extrapolating those results with the observations carried out here, it is possible than in the largest cavities detected in this work the ratio between He and vacancies is lower than 1, indicating possibly bubble-void conversion.

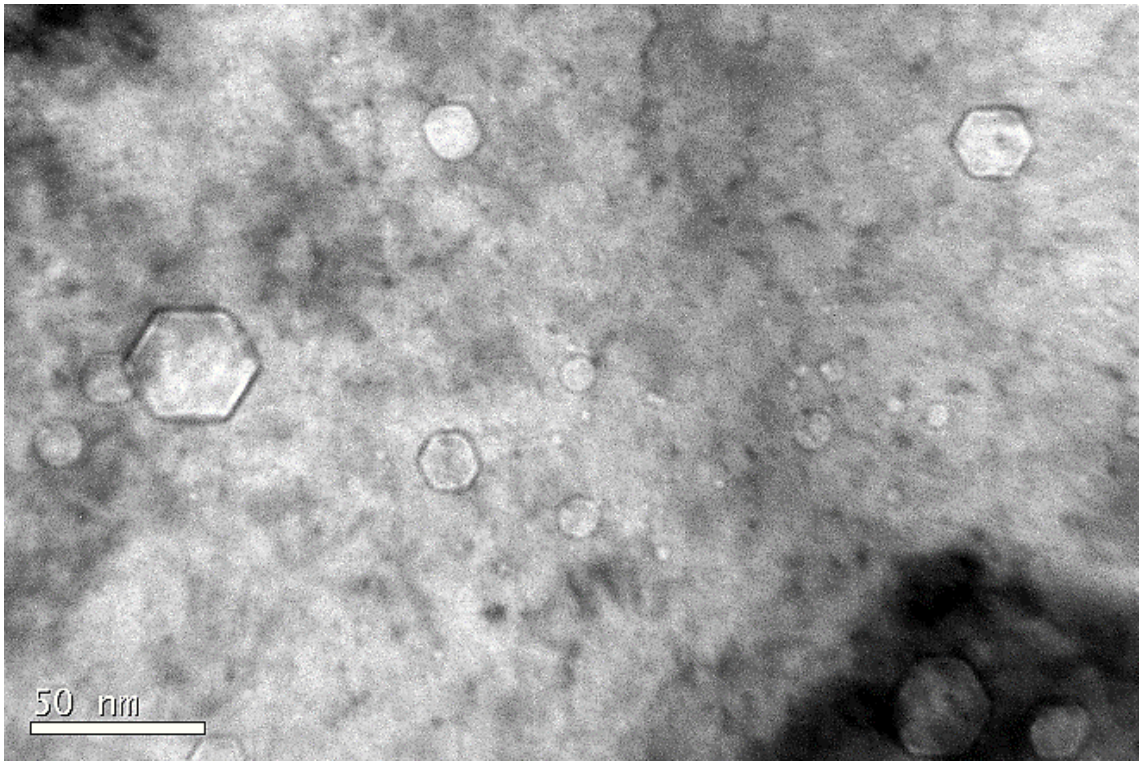

Figure 18 TEM micrograph on bright field underfocused of pure Fe irradiated at 550 ^{o}C, showing different cavities shape.

Due to the difficulty of the experimental observation of diffusion, nucleation and growth of defects produced by helium and hydrogen, together with vacancies and their interaction with microstructural sinks as dislocations or gran boundaries, it is necessary to require modeling studies about it to find a possible explanation of the microstructural observations. In fact the experiment carried out in this research was aimed as experimental back up to modeling studies, since the material used, pure Fe, is one of the most commonly used for modeling because is the base material of the RAFM structural material for the future nuclear fusion reactor.

In any case taking into account modeling results on hydrogen [28-30] and helium [31-33] in form of clusters attached to vacancies (He_nV_m and H_jV_m respectively), it has been reported that both of them tend to stabilize the aforementioned clusters found in the matrix. In fact, it seems that as the amount of gas increases, the binding energy between gas and vacancy also increases. On the other

hand, the iron atoms which belong to the matrix, arranged around the aforementioned cluster are less bounded to their lattice sites, increasing the chances to be emitted into the material as self-interstitial, that is, the loop punching phenomena increased.

However the effect of He and H injected together in the materials makes more difficult the global picture understanding. Again, using modeling results it is observed that there is an interaction between both gases and hence their binding energy to vacancies, interstitials and each other depend strongly on the amount of gas atoms [34]. If the creation of vacancies (dpa) and the injection of interstitials is added to those interactions at the same time (by means of self-ion irradiation) the interpretation of the results is still harder.

Regarding experimental results with triple beams, it has been observed by Tanaka et al. [11] a synergetic effect when introducing simultaneously He, H and Fe ions, explained by an increasing in defect collecting efficiency or in dislocation bias. The microstructural results are clearly different to the observations when double irradiation were performed (Fe+He and Fe+H). In fact, the simultaneous irradiation with Fe and H had no clear effect on swelling increasing. Swelling peak was observed at 510 ^{o}C which is in good agreement with the swelling results obtained in this research; on the other hand, the large cavity detected came from the specimen irradiated at 550 ^{o}C, whose diameter was around 28 nm. The aforementioned synergetic effect between He and H has been observed by E.Wakai [23] in ferritic materials and in vanadium [35] as well.

Y.E. Kupriiyanova et al [36] have observed that both He and H increased the void swelling when the ion gases were introduced separately. However when both ions were implanted simultaneously the effect observed on swelling is different, suggesting a complementary effect, depending on the amount of H injected. If this amount is very high (~1 %) then a suppression in swelling is measured.

Focusing on the microstructural observations it seems that the hydrogen plus helium reduce the critical cavity size or changes the diffusion bias for vacancy accumulation at bubble embryos [37]. Hydrogen, hence, tends to enhance the production of smaller cavities compared to He. This effect is probably due to the greater mobility of H compared to the second one. So, when He and H were injected together the size and population density seem to be biased by He and H keep held in nucleated void.

Although the effect of implanted H on microstructure is very hard to detect, its effect on mechanical properties is proved. For example it reduces the elongation to fracture and produces different phenomena in terms of fracture surface depending on the material [38, 39] among other.

5. CONCLUSIONS

The most important conclusions arising from this research are:

- A novel methodology is presented in this paper in order to improve the quantification of swelling on irradiated materials due to the nucleation of cavities as shown in other experiments

with dual or triple beams setup [40-42]. Since the lamella path was divided into bins (of 250 nm) it is possible to correlate the simulation results in terms of simulated dpa, He and H levels with the microestructural observations.

- Cavities formation at 350 ^{o}C does not match with the expected simulation completely. The largest defects were found in the first 750 nm. Random distribution of small cavities (2 to 4 nm) within the matrix was observed beyond 750 nm.
- Irradiation at 450 ^{o}C and 550 ^{o}C lead to preferential nucleation, being at 550 ^{o}C enhanced to grain boundaries.
- There is a clear temperature effect on cavity growth. As the irradiation temperature increases, the average size of the cavities detected also increases and hence, the volume fraction increases in the implanted region and the maximum peak swelling produced at 550 ^{o}C with a value of 1.4 %.
- The cavities change their morphology at 450 and 550 ^{o}C from round to faceted at a diameter between 16 and 18 nm.
- There are some questions remain about the effect of hydrogen on the stabilization of cavity growth. It turns out that it is necessary to repeat the irradiations but only using He and Fe ion beams and carrying out an exhaustive comparison between the microstructural observations presented in this paper and the further new ones.

6. ACKOWLEDGEMENT

This work was carried out within the framework of the EUROfusion Consortium and has received funding from the Euratom research and training programme 2014-2018 under grant agreement No. 633053. The views and opinions expressed herein do not necessarily reflect those of the European Commission.

7. REFERENCES

1. Y.Dai, G.R. Odette, T.Yammamoto, *The Effects of helium in irradiated structural alloys*, in Comprehensive Nuclear Materials, R.Konings, T.R. Allen, R.E. Stoller, S. Yamanaka Eds. (2012) Elsevier.
2. Fluss, M.J., L.L. Hsiung, and J. Marian, *Dual and Triple Ion-Beam Irradiations of Fe, Fe(Cr) and Fe(Cr)-ODS Final Report: IAEA SMoRE CRP*. 2011.
3. Kim, I.S., et al., *Defect and void evolution in oxide dispersion strengthened ferritic steels under 3.2 MeV Fe+ ion irradiation with simultaneous helium injection.* Journal of Nuclear Materials, 2000. 280(3): p. 264-274.
4. Simons, R.L., H.R. Brager, and W.Y. Matsumoto, *Design of a single variable helium effects experiment for irradiation in FFTF using alloys enriched in nickel-59.* Journal of Nuclear Materials, 1986. 141–143, Part 2: p. 1057-1060.
5. Wakai, E., et al., *Radiation hardening and -embrittlement due to He production in F82H steel irradiated at 250°C in JMTR.* Journal of Nuclear Materials, 2005. 343(1-3): p. 285-296.

6. Hashimoto, N., R.L. Klueh, and K. Shiba, *Pro and cons of Ni and B doping to study helium effects in ferritic martensitic steels.* journal of nuclear materials, 2002. 307-311: p. 7.
7. Yamamoto, T., et al., *The transport and fate of helium in nanostructured ferritic alloys at fusion relevant He/dpa ratios and dpa rates.* Journal of Nuclear Materials, 2007. 367–370, Part A(0): p. 399-410.
8. Dai, Y. and G.S. Bauer, *Status of the first SINQ irradiation experiment, STIP-I.* Journal of Nuclear Materials, 2001. 296(1–3): p. 43-53.
9. Dai, Y., et al., *The second SINQ target irradiation program, STIP-II.* Journal of Nuclear Materials, 2005. 343(1–3): p. 33-44.
10. Krsjak, V., et al., *Helium behavior in ferritic/martensitic steels irradiated in spallation target.* Journal of Nuclear Materials, 2015. 456(0): p. 382-388.
11. Tanaka, T., et al., *Synergistic effect of helium and hydrogen for defect evolution under multi-ion irradiation of Fe–Cr ferritic alloys.* Journal of Nuclear Materials, 2004. 329–333, Part A(0): p. 294-298.
12. Le Coze, J., *Procurement of pure Fe metal and Fe-based alloys with controlled chemical alloying element contents and microstructure*, in *Final report on model alloy preparation*. EFDA – Contract 06 – 1901. TW6 – TTMS 007- PUREFE 2007.
13. Broeders, C.H.M. and A.Y. Konobeyev, *Defect production efficiency in metals under neutron irradiation.* Journal of Nuclear Materials, 2004. 328(2-3): p. 197-214.
14. Shao, L., et al., *Effect of defect imbalance on void swelling distributions produced in pure iron irradiated with 3.5 MeV self-ions.* Journal of Nuclear Materials, 2014. 453(1–3): p. 176-181.
15. Garner, F.A., *Impact of the injected interstitial on the correlation of charged particle and neutron-induced radiation damage.* Journal of Nuclear Materials, 1983. 117: p. 177-197.
16. Brailsford, A.D. and L.K. Mansur, *Effect of self-ion injection in simulation studies of void swelling.* Journal of Nuclear Materials, 1977. 71(1): p. 110-116.
17. Klueh, R.L. and D.R. Harries, *High-chromium ferritic and martensitic steels for nuclear applications*. Monograph. 2001, W. Conshohocken, PA: ASTM. 221 p.
18. Stoller, R.E., *The effect of free surfaces on cascade damage production in iron.* Journal of Nuclear Materials, 2002. 307–311, Part 2: p. 935-940.
19. Aliaga, M.J., M.J. Caturla, and R. Schäublin, *Surface damage in TEM thick α-Fe samples by implantation with 150 keV Fe ions.* Nuclear Instruments and Methods in Physics Research Section B: Beam Interactions with Materials and Atoms, 2015. 352: p. 217-220.
20. Aliaga, M.J., et al., *Surface-induced vacancy loops and damage dispersion in irradiated Fe thin films.* Acta Materialia, 2015. 101: p. 22-30.
21. Getto, E., et al., *Effect of irradiation mode on the microstructure of self-ion irradiated ferritic-martensitic alloys.* Journal of Nuclear Materials, 2015. 465: p. 116-126.
22. Gigax, J.G., et al., *The influence of ion beam rastering on the swelling of self-ion irradiated pure iron at 450 °C.* Journal of Nuclear Materials, 2015. 465: p. 343-348.
23. Wakai, E., et al., *Swelling behavior of F82H steel irradiated by triple/dual ion beams.* Journal of Nuclear Materials, 2003. 318(0): p. 267-273.
24. Trinkaus, H. and B.N. Singh, *Helium accumulation in metals during irradiation – where do we stand? *.* Journal of Nuclear Materials, 2003. 323(2-3): p. 229-242.
25. Fréchard, S., et al., *Study by EELS of helium bubbles in a martensitic steel.* Journal of Nuclear Materials, 2009. 393(1): p. 102-107.
26. Jäger, W., et al., *Density and pressure of helium in small bubbles in metals.* Journal of Nuclear Materials, 1982. 111–112(0): p. 674-680.

27. Slugeň, V., S. Pecko, and S. Sojak, *Experimental studies of irradiated and hydrogen implantation damaged reactor steels.* Journal of Nuclear Materials. http://dx.doi.org/10.1016/j.jnucmat.2015.05.048
28. Hayward, E. and C.S. Deo, *The Energetics of Hydrogen-Vacancy Clusters in BCC Iron.* MRS Online Proceedings Library, 2011. 1363: p. null-null.
29. Irigoyen, B., et al., *The interaction of hydrogen with an Fe vacancy: a molecular orbital simulation.* Journal of Physics D: Applied Physics, 1996. 29(5): p. 1306.
30. Hayward, E. and C.-C. Fu, *Interplay between hydrogen and vacancies in alpha-Fe.* Physical Review B, 2013. 87(17): p. 174103.
31. Lucas, G. and R. Schäublin, *Stability of helium bubbles in alpha-iron: A molecular dynamics study.* Journal of Nuclear Materials, 2009. 386–388(0): p. 360-362.
32. Morishita, K., R. Sugano, and B.D. Wirth, *MD and KMC modeling of the growth and shrinkage mechanisms of helium–vacancy clusters in Fe.* Journal of Nuclear Materials, 2003. 323(2–3): p. 243-250.
33. Morishita, K., et al., *Thermal stability of helium–vacancy clusters in iron.* Nuclear Instruments and Methods in Physics Research Section B: Beam Interactions with Materials and Atoms, 2003. 202(0): p. 76-81.
34. Erin, H. and D. Chaitanya, *Synergistic effects in hydrogen–helium bubbles.* Journal of Physics: Condensed Matter, 2012. 24(26): p. 265402.
35. Sekimura, N., et al., *Synergistic effects of hydrogen and helium on microstructural evolution in vanadium alloys by triple ion beam irradiation.* Journal of Nuclear Materials, 2000. 283–287, Part 1(0): p. 224-228.
36. Kupriiyanova, Y.E., et al., *Use of double and triple-ion irradiation to study the influence of high levels of helium and hydrogen on void swelling of 8–12% Cr ferritic-martensitic steels.* Journal of Nuclear Materials. http://dx.doi.org/10.1016/j.jnucmat.2015.07.012
37. Marian, J., et al., *A review of helium–hydrogen synergistic effects in radiation damage observed in fusion energy steels and an interaction model to guide future understanding.* Journal of Nuclear Materials, 2015. 462(0): p. 409-421.
38. Malitckii, E., Y. Yagodzinskyy, and H. Hänninen, *Hydrogen uptake from plasma and its effect on EUROFER 97 and ODS-EUROFER steels at elevated temperatures.* Fusion Engineering and Design. http://dx.doi.org/10.1016/j.fusengdes.2015.05.049
39. Yagodzinskyy, Y., et al., *Hydrogen effects on tensile properties of EUROFER 97 and ODS-EUROFER steels.* Journal of Nuclear Materials, 2014. 444(1–3): p. 435-440.
40. Brimbal, D., et al., *He and Cr effects on radiation damage formation in ion-irradiated pure iron and Fe–5.40wt.% Cr: A transmission electron microscopy study.* Acta Materialia, 2013. 61(13): p. 4757-4764.
41. Wakai, E., et al., *Effect of triple ion beams in ferritic-martensitic steel on swelling behavior.* Journal of Nuclear Materials, 2002. 307-311: p. 5.
42. Ando, M., et al., *Synergistic effect of displacement damage and helium atoms on radiation hardening in F82H at TIARA facility.* Journal of Nuclear Materials, 2004. 329-333: p. 1137-1141.

FIGURES LIST

TABLE LIST